Nonlinear-optical properties of biexcitons. II. Four-wave mixing

I. Abram
*Centre National d'Etudes des Télécommunications, Laboratoire de Bagneux, 196 rue de Paris, 92220 Bagneux, France**
(Received 31 October 1983)

The nonperturbational treatment for the calculation of the nonlinear-optical susceptibility of an exciton-biexciton system near resonance, developed earlier, is extended to account for multibeam configurations; the case of forward degenerate four-wave mixing is examined in particular. Because of the mutual interactions among the beams, the propagation of each beam in a multibeam configuration is described by a different effective dielectric function: In a pump- and test-beam configuration the renormalization of the polariton dispersion relation near the two-photon biexciton resonance is manifested for the test beam by the opening of a pump-induced polariton gap, while for the strong pump beam itself the dispersion relation displays only a divergence, with no gap. For the parameters of CuCl, the nonperturbational treatment reproduces the main (asymmetric) features of the experimental four-wave-mixing spectrum well. This casts serious doubts on the Fano-interference model for the biexciton, which was previously invoked to reconcile the asymmetric appearance of the spectrum to the perturbational description of four-wave mixing in terms of the third-order susceptibility.

I. INTRODUCTION

The nonlinear-optical spectroscopy of biexcitons in CuCl has commanded a lot of interest in the last few years, both because of the insight which it provides into the electronic states of semiconductors and because of the potential applications associated with the strong optical nonlinearities.[1] Until recently, optical experiments on biexcitons were viewed within the traditional perturbational framework of nonlinear optics. For example, the transmission spectrum[2] and the phase-conjugation (degenerate four-wave mixing) spectrum[3] of CuCl in the vicinity of half the biexciton frequency were regarded as direct manifestations of the third-order susceptibility $\chi^{(3)}$ of the material. Thus deviations from the familiar behavior of $\chi^{(3)}$ observed in these spectra were attributed to novel phenomena: the intensity-dependent width of the two-photon absorption (transmission) spectrum was attributed to collisions within the biexciton gas,[2] while the asymmetry of the phase-conjugation spectrum was explained by invoking an autoionization process for the biexcitons.[3]

The direct experimental observation of many higher-order scattered beams[4] resulting from the interaction of two laser beams near the biexciton resonance in CuCl has demonstrated, however, that the traditional perturbational framework of nonlinear optics is inadequate for the interpretation of optical experiments near the resonances of such systems. This fact casts serious doubts on the perturbational interpretation of nonlinear-optical experiments in CuCl: If the third-order susceptibility $\chi^{(3)}$ does not suffice to describe two-photon absorption and four-wave mixing, then the evidence for collisional and autoionizing phenomena in biexcitons needs to be revised.

Several authors have calculated the nonlinear-optical dielectric function of CuCl in the vicinity of the two-photon biexciton resonance through nonperturbational methods, thus obtaining the intensity-dependent renormalization of the polariton-dispersion relation.[5,6] In a recent publication[7] (hereafter referred to as I) we developed a nonperturbational technique for the calculation of the nonlinear-optical polarizability based on the determination of the unitary transformation that diagonalizes the exciton-biexciton—radiation Hamiltonian. The nonlinear dielectric function thus obtained is exact within the rotating wave approximation (i.e., it includes all fully resonant terms of all orders of the susceptibility), and reduces to the expressions found by other authors under the appropriate approximations. By treating light propagation also in a nonperturbational framework, we showed that at least part of the intensity-dependent width of the biexciton resonance, observed in transmission experiments, is due to the frequency displacement of the intensity-dependent biexciton resonance (chirping) as the transmitted beam is absorbed while it propagates. If biexciton collisions cause additional broadening, the effect of this latter mechanism will be intertwined with the apparent broadening due to chirping.

A dielectric function, however, calculated for the propagation of a single beam cannot take into account the interaction between different light beams propagating in the same medium. In the perturbational language of nonlinear optics, this nonlinear dielectric function incorporates only the intensity-dependent renormalization of the first-order susceptibility and can be used therefore only for the description of the most elementary optical-nonlinear experiments: those involving a single light beam, such as transmission or reflection spectroscopy. The more interesting experimental situations involving several beams such as state-preparation and probing setups or n-wave-mixing configurations require the calculation of the renormalization of the $(n-1)$th order susceptibility and cannot be accounted for through the one-beam dielectric function. The nonperturbational description of four-wave mixing using the density-matrix formalism has

recently been addressed by several authors.[8,9]

In this paper we generalize the treatment of paper I to address the problem of the nonlinear-optical response of an exciton-biexciton system in a general n-beam configuration. In order to make contact with experimental observations, we specialize our treatment to the description of forward degenerate four-wave mixing in CuCl. This paper is organized as follows: In Sec. II we review the basic ideas of paper I while at the same time we recast them in a generalized framework which permits the treatment of multibeam experiments. In Sec. III we apply our theory to degenerate four-wave mixing and analyze previous experimental results in the light of this theory. Finally, Sec. IV contains a summary of our results and a discussion of the nonperturbational approach.

II. MODEL

A. Hamiltonian

We consider a semiconductor interacting with n distinct laser beams, all at the same frequency ω, in near resonance with the exciton and with the two-photon biexciton transitions. We assume, however, that the beams may be distinguished through their directions of propagation, so that each may be represented by a plane-wave electric field

$$E_j e^{i\omega t - ik_j r} + E_j^* e^{-i\omega t + ik_j r} . \tag{2.1}$$

As in paper I, the electromagnetic field is expressed classically while the electronic states of the crystal are treated quantum mechanically. The resonance condition permits us to ignore most electronic states of the semiconductor and to write the semiconductor Hamiltonian as involving only two types of quasiparticles: excitons and biexcitons, which are both bosons. Then

$$H_0 = \sum_q \omega_0(q) b_q^\dagger b_q + \sum_Q \Omega(Q) B_Q^\dagger B_Q , \tag{2.2}$$

where $b_q^\dagger/b_q$ ($B_Q^\dagger/B_Q$) are the creation and annihilation operators for excitons (biexcitons) of wave vector q (Q) and frequency ω (Ω). These operators follow Bose commutation relations. Absorption of a photon of wave vector k_j may create an exciton of the same wave vector, or it may create a biexciton of wave vector k_j+q if an exciton of wave vector q is already present (actually or virtually) in the crystal. Thus, the interaction Hamiltonian between the crystal and the jth beam is

$$\begin{aligned} H_j = &-\sqrt{N}\mu_1 (E_j e^{-i\omega t} b_{k_j}^\dagger + E_j^* e^{i\omega t} b_{k_j}) \\ &-\mu_2 \sum_q (E_j'^* e^{-i\omega t} B_{q+k_j}^\dagger b_q \\ &+ E_j'^* e^{i\omega t} B_{q+k_j} b_q^\dagger) , \end{aligned} \tag{2.3}$$

where μ_1 is the exciton transition dipole per unit cell, N is the number of unit cells in the crystal, and μ_2 is the exciton-biexciton transition dipole. A prime E' is used to indicate the possibility that the exciton and the biexciton do not feel exactly the same field, due to the "local-field" contribution: As discussed in paper I, if in CuCl only the exciton is subject to the local field (while the biexciton feels directly the applied external field), inclusion of the local field produces simply a constant shift of the exciton frequency in the calculation of the nonperturbational susceptibility. Under the same assumptions, it can be shown that the same effect occurs in multibeam configurations. For this reason the prime in Eq. (2.3) will be dropped, and local-field effects will not be explicitly considered in this paper.

The Hamiltonian of a crystal interacting with n distinct beams is

$$H = H_0 + \sum_{j=1}^n H_j . \tag{2.4}$$

Clearly, the wave vectors of the excitons and biexcitons entering in Eq. (2.4) must satisfy the same conservation relations that may exist among the wave vectors of the light beams as imposed by the experimental geometry. Since the individual interaction Hamiltonians H_j are quadratic in the exciton and biexciton operators, the unitary transformation that diagonalizes (2.4) may be obtained in analytical form. The diagonalization procedure is easiest if the oscillatory time dependence of the interaction Hamiltonian is eliminated through a rotating-frame transformation analogous to that used in nuclear magnetic resonance. Since there are two resonances involved, a double rotating frame must be used, one for the excitons rotating at frequency ω and one for the biexcitons rotating at 2ω. The Hamiltonian in this frame is

$$\tilde{H} = \tilde{H}_0 + \sum_{j=1}^n \tilde{H}_j , \tag{2.5a}$$

$$\tilde{H}_0 = \sum_q \delta(q) b_q^\dagger b_q + \sum_Q \Delta(Q) B_Q^\dagger B_Q , \tag{2.5b}$$

$$\begin{aligned} \tilde{H}_j = &-\sqrt{N}\mu_1 (E_j b_{k_j}^\dagger + E_j^* b_{k_j}) \\ &-\mu_2 \sum_q (E_j B_{q+k_j}^\dagger b_q + E_j^* B_{q+k_j} b_q^\dagger) , \end{aligned} \tag{2.5c}$$

with $\delta(q)=\omega_0(q)-\omega$ and $\Delta(Q)=\Omega(Q)-2\omega$. The unitary transformation may now be written as the product of two successive partial transformations each diagonalizing part of the Hamiltonian. First, a translational transformation U_1 is used such that

$$U_1 b_q U_1^{-1} = b_q + x_q , \tag{2.6a}$$

$$U_1 B_Q U_1^{-1} = B_Q + y_Q \tag{2.6b}$$

(and the complex conjugates for the creation operators). The parameters x_q and y_Q are then chosen so that the linear terms in the exciton operators ($b_q + b_q^\dagger$) are eliminated in Eq. (2.5). Second, a rotational transformation is used, such that

$$U_2 b_{q'} U_2^{-1} = \sum_q \alpha_{q'q} b_q + \sum_Q \beta_{q'Q} B_Q , \tag{2.7a}$$

$$U_2 B_{Q'} U_2^{-1} = \sum_q \alpha'_{Q'q} b_q + \sum_Q \beta'_{Q'Q} B_Q \tag{2.7b}$$

eliminates the quadratic cross terms ($B^\dagger b + B b^\dagger$) in $\tilde{H}_j$. The overall unitary transformation is given by

$$U = U_2 U_1 . \tag{2.8}$$

B. Nonlinear polarization

The electromagnetic fields propagating in the medium induce an oscillating polarization which in turn may emit radiation similar to a classical antenna, according to Maxwell's equations. Thus, in order to account for the experimental observation of a light beam of frequency ω and wave vector k generated and propagating through the material, it is necessary to calculate the induced polarization of the same frequency and wave vector. In this calculation, all transitions which may produce a photon in the k direction must be included. Thus the polarization relevant to an experimental observation is given by the expectation value of the (ω,k) component of the dipole operators for *both* the ground-to-exciton and the exciton-to-biexciton transitions

$$\hat{\mu}(\omega,k)=\sqrt{N}\mu_1 b_k e^{i\omega t}+\mu_2\sum_q B_{k+q}b_q^{\dagger}e^{i\omega t} \tag{2.9}$$

over the state in which the system is found after the field is turned on adiabatically. The expectation value of the first term gives the probability that the photon emitted by the oscillating induced polarization is associated with the annihilation of an exciton, while the second term gives the probability that the emission of a photon takes place when the crystal undergoes a biexciton-to-exciton transition. Clearly, calculations that neglect this latter term[5] cannot adequately describe the optical response of biexcitons especially at high intensities.

By using the unitary transformation U that diagonalizes the Hamiltonian in the double rotating-frame representation, the amplitude of the induced polarization may be written as

$$P(\omega,k)=V^{-1}\langle n \mid U\hat{\mu}'U^{-1}\mid n\rangle , \tag{2.10a}$$

where V is the volume of the crystals, $|n\rangle$ is the initial state of the system, while $\hat{\mu}'$ is the same as Eq. (2.9) but with the oscillatory time dependence suppressed. We note that if the initial state of the crystal contains no excitons or biexcitons, i.e., $|n\rangle=|0\rangle$ the rotational part of the unitary transformation gives no contribution as was shown in paper I,

$$\begin{aligned}P(\omega,k)&=V^{-1}\langle 0\mid U_2U_1\hat{\mu}'U_1^{-1}U_2^{-1}\mid 0\rangle\\&=V^{-1}\langle 0\mid U_1\hat{\mu}'U_1^{-1}\mid 0\rangle .\end{aligned} \tag{2.10b}$$

Thus, in such a case, the translational part of the unitary transformation is sufficient for the calculation of the induced polarization.

The induced polarization is created by the nonlinear interaction of the electromagnetic fields, but is destroyed by the relaxation processes that take place in the crystal. The steady-state value of the polarization amplitude may be obtained by adding a small imaginary part to all frequencies in Eq. (2.10), positive for creation operators, negative for annihilation operators, and equal to the decay constant of the corresponding state. In particular, the detunings become

$$\delta(q)\rightarrow\delta(q)\pm i\gamma ,$$
$$\Delta(Q)\rightarrow\Delta(Q)\pm i\Gamma ,$$

where γ and Γ are transition-dipole damping constants for the exciton and the biexciton, respectively.

C. Nonlinear propagation

In multibeam experiments the Maxwell equations can be written as a series of propagation equations, one for each beam. The steady-state propagation equation for the jth beam in a material system may be written as

$$\frac{\partial^2E_j}{\partial z^2}=-\frac{\omega^2}{c^2}[E_j+4\pi P(\omega,k_j)] , \tag{2.11}$$

where $P(\omega,k_j)$ is the steady-state amplitude of the (ω,k_j) component of the induced polarization which depends in general on the values of all the fields present. We may formally separate P into two parts:

$$P(\omega,k_j)=\eta_j(E_i)+\chi_j(E_i,E_j)E_j , \tag{2.12}$$

the first part (η_j) is independent of E_j but depends on all other fields (denoted by E_i) in the medium, while the second part depends on the value of E_j as well as the values of the other fields. This partition of P permits us to rewrite Eq. (2.11) as

$$\frac{\partial^2E_j}{\partial z^2}=-\frac{\omega^2}{c^2}(\epsilon_jE_j+4\pi\eta_j) , \tag{2.13a}$$

where we have defined

$$\epsilon_j=1+4\pi\chi_j \tag{2.13b}$$

which plays the role of an effective dielectric function experienced by the jth beam during its propagation but depends on the presence of all fields. The term in η_j plays the role of a source term and causes the emission of radiation E_j, as from a classical antenna. We note that both ϵ_j and η_j are in principle different for different beams propagating in the same medium.

For the case in which ϵ_j and η_j do not vary greatly with distance, as for example when the intensities of all fields involved do not decrease (due to absorption) or increase (due to generation or amplification) too fast, the second-order propagation equation (2.13) can be reduced into a first-order equation. In particular, when $\eta_j=0$, following the same procedure as in paper I, the propagation equation may be approximated by

$$\frac{\partial E_j}{\partial z}=ik_jE_j , \tag{2.14a}$$

where

$$k_j=\frac{\omega}{c}\sqrt{\epsilon_j} \tag{2.14b}$$

is the wave vector. These equations are valid when

$$\left|\frac{\partial}{\partial z}\frac{1}{k_j}\right|\ll 1 , \tag{2.15}$$

that is, when the wavelength varies slowly, so that a wave vector can be defined locally. Under the same conditions, the full equation with the source term may be written as

$$\frac{\partial E_j}{\partial z}=ik_jE_j+4\pi i\frac{\omega}{c}\frac{\eta_j}{\sqrt{\epsilon_j}} . \tag{2.16}$$

This equation is exact only when ϵ_j and η_j do not depend on z. It is, however, a good approximation to the full propagation equation, as can be verified by redifferentiating Eq. (2.16), when condition (2.15) is satisfied, and at the same time

$$\left| \frac{1}{k_j \eta_j} \frac{\partial}{\partial z} \eta_j \right| \ll 1 , \tag{2.17}$$

that is, when the variation of the amplitude of the source term is small over one wavelength.

III. FOUR-WAVE MIXING

We now examine the forward configuration of degenerate four-wave mixing, as described in the experimental papers of Chemla and co-workers.[3,4] In these experiments, the CuCl crystal is initially in its ground state, and interacts with a strong laser beam (pump) of wave vector k_0 and a weaker beam (test) of the same frequency and of wave vector k_{-1} to produce a series of scattered beams emerging in the directions

$$k_n = (n+1)k_0 - nk_{-1} . \tag{3.1}$$

However, when the test beam is very weak, only the first scattered beam ($n=1$) is observed, and the four-wave mixing configuration is realized. Clearly, in the description of this process the test field is included only up to first order while the pump field must be treated nonperturbationally. The response of the material, thus, can be expressed by the $\chi^{(3)}$ corresponding to four-wave mixing, renormalized, however, for the high intensity of the pump beam. It is this simpler problem that we address in this paper, by limiting our calculation to the beams corresponding to $n=0$ and $n=\pm 1$. Inclusion of higher-order scattered beams ($n=\pm 2, \pm 3, \ldots,$) and the full nonperturbational description of the phenomenon can easily be achieved following the procedure we develop for four-wave mixing; however, even though this is conceptually straightforward within our formalism, the corresponding algebra is rather tedious. Furthermore, we examine only the case in which there is no initial exciton or biexciton population in the sample, since this case corresponds to the experimental conditions while at the same time it simplifies the calculation of the unitary transformation that diagonalizes the Hamiltonian.

Within the four-wave mixing configuration, it is reasonable to assume that the relative intensities of the fields involved are

$$|E_0|^2 \gg |E_{-1}|^2 \gg |E_1|^2 , \tag{3.2}$$

and thus we may ignore all transitions involving more than one test or signal photons. We therefore take into account all one-photon transitions and only those two-photon transitions that involve (1) two-pump photons, (2) a pump plus a test photon, and (3) a pump plus a signal photon. Since there are initially no excitons or biexcitons present in the crystal, the wave-vector conservation rules limit the interaction of the radiation field to excitons of wave vector k_0 and $k_{\pm 1}$ and to biexcitons of total wave vector $K_0 = 2k_0 = k_1 + k_{-1}$, $K_{-1} = k_0 + k_{-1}$, and $K_1 = k_0 + k_1$. The biexciton K_0 is directly involved in the two-photon absorption of the pump beam and in the four-wave mixing process, while the two others result from the absorption on the test or signal beams induced by the presence of the pump beam. In keeping with the assumption (3.2) we neglect biexcitons of wave vector $K_{\pm 2} = 2k_{\pm 1}$ involved in the two-photon absorption of the test and signal beams. The Hamiltonian corresponding to this situation in the double rotating frame of reference is

$$H = \delta b_0^\dagger b_0 + \Delta B_0^\dagger B_0 - \sqrt{N}\mu_1(E_0 b_0^\dagger + E_0^* b_0) - \mu_2(E_0 B_0^\dagger b_0 + E_0^* B_0 b_0^\dagger) \tag{3.3a}$$

$$+ \delta b_{-1}^\dagger b_{-1} - \sqrt{N}\mu_1(E_{-1} b_{-1}^\dagger + E_{-1}^* b_{-1}) - \mu_2(E_{-1} B_0^\dagger b_1 + E_{-1}^* B_0 b_1^\dagger) \tag{3.3b}$$

$$+ \delta b_1^\dagger b_1 - \sqrt{N}\mu_1(E_1 b_1^\dagger + E_1^* b_1) - \mu_2(E_1 B_0^\dagger b_{-1} + E_1^* B_0 b_{-1}^\dagger) \tag{3.3c}$$

$$+ \Delta B_{-1}^\dagger B_{-1} - \mu_2(E_0 B_{-1}^\dagger b_{-1} + E_0^* B_{-1} b_{-1}^\dagger) \tag{3.3d}$$

$$- \mu_2(E_{-1} B_{-1}^\dagger b_0 + E_{-1}^* B_{-1} b_0^\dagger) \tag{3.3e}$$

$$+ \Delta B_1^\dagger B_1 - \mu_2(E_0 B_1^\dagger b_1 + E_0^* B_1 b_1^\dagger) \tag{3.3f}$$

$$- \mu_2(E_1 B_1^\dagger b_0 + E_1^* B_1 b_0^\dagger) , \tag{3.3g}$$

where we have taken $\delta(k_0) = \delta(k_{-1}) = \delta(k_1) = \delta$ and $\Delta(K_0) = \Delta(K_{-1}) = \Delta(K_{-1}) = \Delta$ which is rigorously justified for cubic crystals. The first line of this Hamiltonian, Eq. (3.3a), is identical to the Hamiltonian examined in paper I: It describes the interaction of the pump beam alone with the crystal, and involves the excitons k_0 (through one-photon transitions) and the biexcitons K_0 (through two-photon or two-step transitions). The interaction of the crystal with the two other beams is described in Eqs. (3.3b)–(3.3g). In particular, Eqs. (3.3b) and (3.3c) describe the one-photon interaction of the test and signal beams with the crystal, through the corresponding exciton transition, as well as the two-photon interaction which gives rise to four-wave mixing through the deexcitation of a K_0 biexciton by the emission of one test and one signal photons: The last term of Eq. (3.3c) corresponds to the case in which the signal photon is emitted during the biexciton-to-exciton transition, whereas in the last term of Eq. (3.3b) it is the test photon that is emitted in this transition while the signal photon is associated with the exciton-to-ground part of the two-photon transition. Equations (3.3d) and (3.3e) involve the K_{-1} biexciton and thus describe the test-beam absorption induced by the presence of the pump beam: in Eq. (3.3e) a test photon is involved in the exciton-to-biexciton transition, whereas in Eq. (3.3c) the test photon is associated with the ground-

to-exciton step. Similarly, Eqs. (3.3f) and (3.3g) describe the induced absorption of the signal beam giving rise to the K_1 biexciton.

The Hamiltonian (3.3) may be diagonalized according to the procedure outlined in Sec. II A. For our purposes and for a crystal initially in its ground electronic state it is sufficient to calculate only the translational part of the unitary transformation, as shown in paper I. Introducing Eqs. (2.6) into Eqs. (3.3), we may calculate the values of the parameters x_i and y_i which define a translational unitary transformation such that the linear terms of Eqs. (3.3) are eliminated. The system of simultaneous linear equations that results from this substitution is

$$\begin{array}{cccccc} \delta x_0 & +0 & +0 & -\mu_2 E_0^* y_0 & -\mu_2 E_{-1}^* y_{-1} & -\mu_2 E_1^* y_1 = \sqrt{N}\mu_1 E_0 \quad (3.4a) \\ 0 & +\delta x_{-1} & +0 & -\mu_2 E_1^* y_0 & -\mu_2 E_0^* y_{-1} & +0 = \sqrt{N}\mu_1 E_{-1} \quad (3.4b) \\ 0 & +0 & +\delta x_1 & -\mu_2 E_{-1}^* y_0 & +0 & -\mu_2 E_0^* y_1 = \sqrt{N}\mu_1 E_1 \quad (3.4c) \\ -\mu_2 E_0 x_0 & -\mu_2 E_1 x_{-1} & -\mu_2 E_{-1} x_1 & +\Delta y_0 & +0 & +0 = 0 \quad (3.4d) \\ -\mu_2 E_{-1} x_0 & -\mu_2 E_0 x_{-1} & +0 & +0 & +\Delta y_{-1} & +0 = 0 \quad (3.4e) \\ -\mu_2 E_1 x_0 & +0 & -\mu_2 E_0 x_1 & +0 & +0 & +\Delta y_1 = 0 \quad (3.4f) \end{array}$$

In keeping with our assumptions on the relative strengths of the three radiative fields we may solve Eqs. (3.7) only up to first order in $E_{\pm 1}$, but to all orders in E_0.

The calculation of the generation and propagation of each beam in the crystal involves the induced polarization of the corresponding wave vector, as in Eqs. (2.9) and (2.10). For the pump beam, this polarization is given by the expectation value over the adiabatic state of the dipole operator of all transitions involving a pump photon. These are the one-photon k_0-exciton transition, the k_0-exciton—to—K_0-biexciton transition, and the pump-induced absorption of the test and signal beams. That is

$$\hat{\mu}(k_0)=\sqrt{N}\mu_1 b_0+\mu_2 B_0 b_0^\dagger+\mu_2 B_{-1} b_{-1}^\dagger+\mu_2 B_1 b_1^\dagger \, . \quad (3.5a)$$

For the signal beam, the corresponding dipole operator involves the k_1 exciton, the test-and-signal deexcitation of the K_0 biexciton (four-wave mixing), and the pump-induced absorption of the signal beam, giving thus

$$\hat{\mu}(k_1)=\sqrt{N}\mu_1 b_1+\mu_2 B_0 b_{-1}^\dagger+\mu_2 B_1 b_0^\dagger \, , \quad (3.5b)$$

while for the test beam the dipole operator $\hat{\mu}(k_{-1})$ has the same form as Eq. (3.5b) but with the indices ± 1 interchanged. The induced polarization interacting with each beam may be obtained by combining Eqs. (2.10), (2.6), and (3.5) as

$$P(k_0)=V^{-1}(\sqrt{N}\mu_1 x_0+\mu_2 y_0 x_0^*+\mu_2 y_{-1} x_{-1}^*+\mu_2 y_1 x_1^*) \quad (3.6a)$$

and

$$P(k_1)=V^{-1}(\sqrt{N}\mu_1 x_1+\mu_2 y_0 x_{-1}^*+\mu_2 y_1 x_0^*) \, . \quad (3.6b)$$

The expression for $P(k_{-1})$ is similar to Eq. (3.6b) with the indices ± 1 interchanged. Inserting now the solutions of Eqs. (3.4) into Eqs. (3.6) and taking into account the relative intensities of the fields involved (3.2), we obtain for the pump beam

$$P(k_0)=\chi_0(E_0)E_0 \quad (3.7a)$$

with

$$\chi_0(E_0)=\frac{N}{V}\mu_1^2\frac{(\Delta\Delta^*\delta^*+2i\Gamma R^2)}{|\Delta\delta-R^2|^2} \, , \quad (3.7b)$$

where $R=|\mu_2 E_0|$ is the Rabi frequency of the exciton-biexciton transition driven by the pump beam. For the signal beam we have

$$P(k_1)=\eta_1(E_0,E_{-1})+\chi_1(E_0)E_1 \, , \quad (3.8a)$$

where

$$\eta_1(E_0,E_{-1})=-\frac{N\mu_1^2\mu_2^2}{V}\left[\frac{\Delta}{(\Delta\delta-R^2)^2}+\frac{\Delta^*}{|\Delta\delta-R^2|^2}\left[\frac{\Delta\delta}{\Delta\delta-R^2}+\frac{R^2}{\Delta^*\delta^*-R^2}\right]\right]E_0 E_0 E_{-1}^* \quad (3.8b)$$

and

$$\chi_1(E_0)=\frac{N\mu_1^2}{V}\left[\frac{\Delta^2\delta}{(\Delta\delta-R^2)^2}+\frac{\Delta^* R^2}{|\Delta\delta-R^2|^2}\left[\frac{\Delta\delta}{\Delta\delta-R^2}+\frac{\Delta^*\delta^*}{\Delta^*\delta^*-R^2}\right]\right] \, , \quad (3.8c)$$

while for the test beam the indices ± 1 are interchanged in Eqs. (3.8).

For the sake of clarity, the induced polarization (3.8) was partitioned formally into two terms, as in Sec. II C. This separation permits a better understanding of the role of the induced polarization in the Maxwell equations. The first term, η, is independent of the field E_j and thus serves as a source term for the generation of the jth beam in the Maxwell equations. In the perturbational language of nonlinear optics, this term can be expressed as the third-order susceptibility relevant to four-wave mixing renormalized by all higher-order virtual transitions involving the pump beam, in addition to four-wave mixing. In the second term, the quantity $\chi_j(E_0)$ of Eq. (3.8c) as well as the corresponding $\chi_0(E_0)$ of Eq. (3.7b) represents the renormalization of the first-order susceptibility seen by

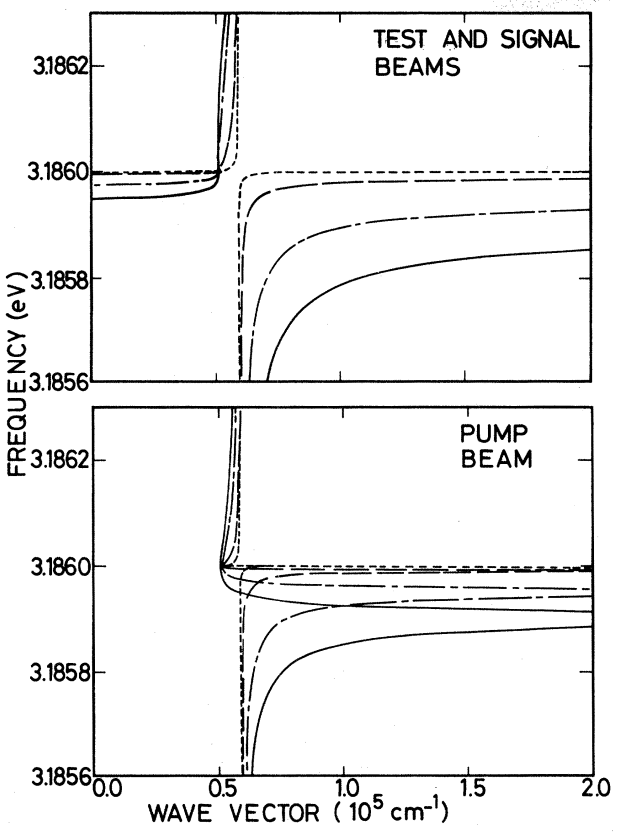

FIG. 1. Polariton-dispersion relations near the biexciton resonance of CuCl (3.186 eV) with no damping, renormalized by a strong pump beam. Upper curve: polariton renormalization induced on a weak (test or signal) beam. Lower curve: self-renormalization of pump-beam polariton dispersion. Solid line (——) is for an internal pump field of 500 esu, dashed-dotted line (-·-·-) is for 350 esu, long-dashed line (—) is for 150 esu, and short dashes (- - - -) are for 50 esu.

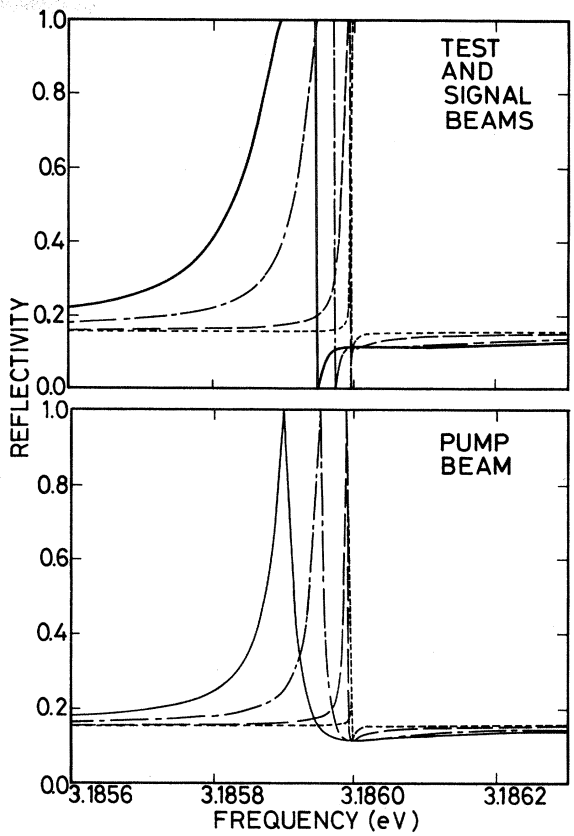

FIG. 2. Reflectivity of CuCl in the vicinity of the two-photon biexciton resonance (3.186 eV) with no damping, for two incident beams: a high-intensity (pump) and a low-intensity (test) beam. Curves are for different internal pump fields, as in Fig. 1. Test beam displays a polaritonlike gap, while the pump beam exhibits divergence (the reflectivity is equal to 1) at only one point.

the jth beam (as it propagates in the material) due to the intensity of the pump beam and the occurrence of the exciton-to-biexciton transition. The real and imaginary parts of $\chi_j(E_0)$ correspond to the dispersive and absorptive coefficients felt by the jth beam during its propagation in the system composed of the material plus the pump beam. When the induced polarization is inserted in the Maxwell equations, $\chi_j(E_0)$ gives rise to $\epsilon_j(E_0)$, the effective dielectric function of the medium seen by the jth beam in the presence of the pump beam,

$$\epsilon_j(E_0)=\epsilon_\infty+4\pi\chi_j(E_0)\ , \tag{3.9}$$

where ϵ_∞ is the background dielectric function due to all electronic states other than the exciton and the biexciton. It should be noted that the value of the different electric fields entering in Eqs. (3.2)—(3.9) are to be taken inside the material. Near the air (or vacuum) interface, these fields may be related to the incident intensities through the transmission coefficient

$$E_j=\frac{2}{1+\sqrt{\epsilon_j}}E_j^{\rm inc}=\frac{2}{1+\sqrt{\epsilon_j}}\left[\frac{8\pi I_j^{\rm inc}}{c}\right]^{1/2}\ . \tag{3.10}$$

Thus, in order to express the nonlinear susceptibilities in terms of the incident intensities, Eqs. (3.7) and (3.10) must be solved self-consistently.

A few comments on the dielectric functions seen by the three beams are in order. The dielectric function seen by the pump beam $\epsilon_0(E_0)$ and Eq. (3.7) are identical to the corresponding expressions obtained in paper I for a single incident beam propagating through the material. This is due to the fact that all calculations are performed to infinite order for the pump field but only to first order for the test and signal fields: There is no first-order contribution of these latter fields to $\chi_0(E_0)$. On the other hand, the dielectric functions seen by the test and signal beams $\epsilon_{-1}(E_0)$ and $\epsilon_1(E_0)$ are identical to each other, but have a different functional form from $\epsilon_0(E_0)$. This implies that optical measurements of the material done in one-beam experiments or in two-beam pump-and-test configurations do not give the same results. In particular, the renormalization of the polariton-dispersion relation in the vicinity of the two-photon biexciton resonance is seen quite differently by the pump and by the test beams: In a one-beam experiment (or for the pump beam of a two-beam configuration) this renormalization is manifested by the

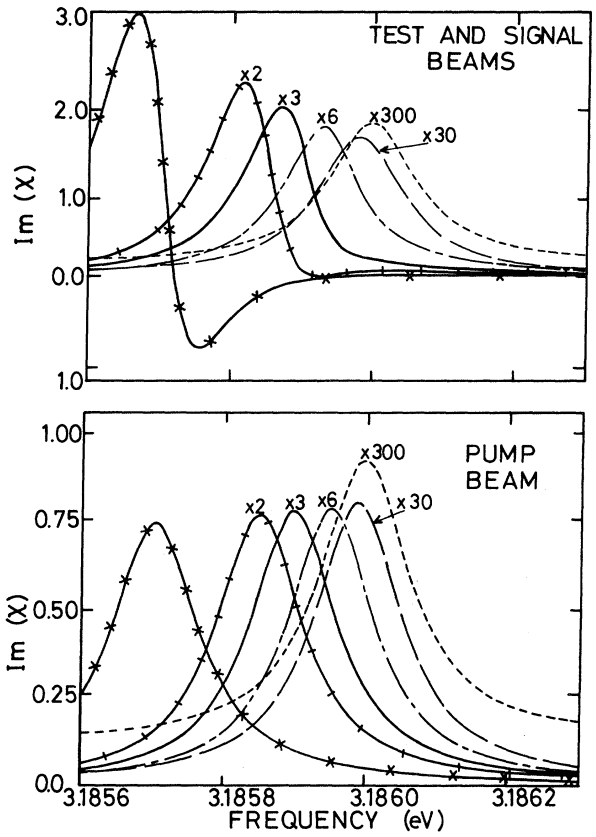

FIG. 3. Imaginary part of the optical susceptibility of CuCl in the vicinity of the two-photon biexciton resonance for two incident beams: a high-intensity (pump) and a low-intensity (test) beam. Damping constants are $\gamma=0.07$ and $\Gamma=0.15$ meV. Curves are for different internal pump fields: $\times$ is for a field of 900 esu, $+$ is for 650 esu, and the rest are as in Fig. 1. At high intensities Imχ corresponding to the test beam may be negative, indicating amplification.

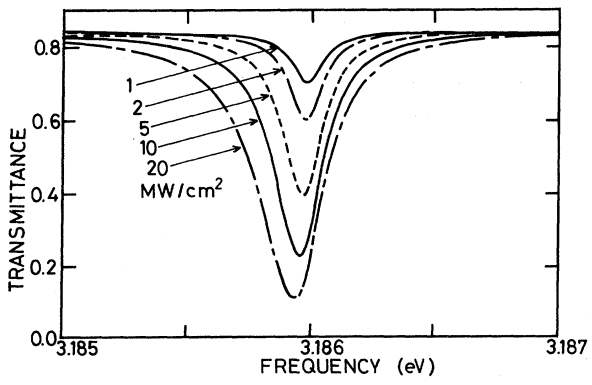

FIG. 4. Calculated transmission spectra of a weak test beam in the presence of a high-intensity pump beam near the two-photon biexciton absorption of a 0.5-μm film of CuCl. Curves are for different incident pump intensities.

divergence of the polariton dispersion at *only one point,* whose spectral position varies essentially as the square of the pump field inside the material, and is given approximately by

$$\omega_r \approx (\Omega - R^2/\delta)/2 \,. \tag{3.11}$$

This gives rise to a relatively sharp peak in the reflectivity of the material at ω_r for a constant transmitted pump field E_0. On the other hand, in a two-beam experiment the test beam measures a qualitatively different polariton dispersion: The system composed of the material plus the pump beam exhibits a *polariton gap,* that is, a spectral region in which the test beam cannot enter the crystal because $\epsilon_{-1}(E_0)$ is negative and the corresponding renormalized refractive index is purely imaginary. The reflectivity seen by the test beam in the presence of the pump beam presents, therefore, a region in which it reaches the value of 1 (one), corresponding to the pump-induced opening of the polariton gap. For the parameters of CuCl (Refs. 10 and 11) ($\omega_0=3.204$, $\Omega=6.372$ eV; $\epsilon_\infty=4.1$, $\mu_2=10^{-17}$ esu, and a longitudinal-transverse splitting of $\omega_{LT}=N\mu_1^2/V\epsilon_\infty=5.4$ meV) this gap extends from ω_r to approximately $(\omega_r+\Omega/2)/2$ for intensities of up to a few tens of MW/cm^2; its position and width, thus, vary with the pump beam. A pump-induced polariton gap in CuCl has recently been observed[12] in hyper-Raman experiments. Although the present calculation is not applicable, strictly speaking, to such multifrequency configurations, we may expect its conclusions to hold qualitatively even when the pump, test, and signal frequencies are all different, as in hyper-Raman scattering. A comparison of the polariton-dispersion relations and the corresponding reflectivities seen by the pump and test beams, when no dissipative effects are present in the crystal, is shown in Figs. 1 and 2. These curves are calculated at a constant internal field, rather than at a constant incident intensity; that is, the transmission coefficient of Eq. (3.10) is not taken into account. The reason is that when no damping is included, the self-consistent solution of Eqs. (3.7) and (3.10) cannot converge near resonance. Please note that also in paper I Figs. 1 and 2 were calculated without the self-consistent correction for the transmission coefficient; consequently, the intensities identified in the figures correspond to the squares of the internal fields, and not to the incident intensities.

The origin of the difference in the dispersion relations can be traced to the distinguishability of the beams participating in the two types of processes. As noted in Sec. II B and Eqs. (3.5) the induced polarization is the sum of all elementary processes in which there is a net emission of one photon. The dielectric function seen by the test beam includes all elementary processes which involve one test photon along with several pump photons: The pump photons are emitted and reabsorbed and the net result is the emission of the test photon. The induced polarization has also another component which is linear in the test-beam field: it involves all elementary processes in which one test photon is absorbed but two pump photons are emitted (along with any number of virtual emissions and reabsorptions of pump photons) so that the net result is still the emission of one photon. This latter component of the induced polarization, however, does not contribute to

the test-beam dielectric function but is included in the source term for the signal beam (η_1). On the other hand, for the pump beam (or for single-beam propagation) the induced polarization includes all elementary processes in which only pump photons participate, with the net result being, of course, the emission of one pump photon. As the pump photons cannot be distinguished among them, the two separate contributions which for the test (and signal) beam yield χ_j and η_j, both enter in the determination of the pump-beam susceptibility. Indeed, it is easy to verify that when $k_0=k_1=k_{-1}$, that is, when the pump, test, and signal beams cannot be distinguished so that $E_0=E_1=E_{-1}=E$ Eqs. (3.7) and (3.8) give identical results. That is,

$$\chi_1(E)E+\eta_1=\chi_0(E)E\ , \tag{3.12}$$

where the indices are used simply to denote the different functional forms.

When relaxation processes are included, the susceptibilities and the corresponding dielectric functions acquire an imaginary part. This causes the polariton-dispersion relation to be modified: The polariton divergence of $\epsilon_0(E_0)$ and the polariton gap of $\epsilon_1(E_0)$ disappear. At the same time, the reflectivity peaks due to this polariton effect become greatly attenuated.

For the pump beam, the imaginary part of the nonperturbational susceptibility $\chi_0(E_0)$ is always positive, indicating that this beam can be only attenuated when it propagates in the crystal. The maximum of $\mathrm{Im}\chi_0$ shifts to lower frequencies by an amount essentially proportional to the incident intensity. On the other hand, the imaginary part of the test-beam susceptibility $\chi_{-1}(E_0)$ may take negative values for sufficiently strong pump fields as shown in Fig. 3. This occurs when

$$R^2>[(\Omega-2\omega)^2+\Gamma^2]\frac{\omega_0-\omega}{(\Omega-2\omega)} \tag{3.13}$$

as can be seen from Eq. (3.8c) after some algebra. In this case, the test beam is amplified when it propagates in the presence of the pump beam. This behavior may be easily understood if we consider the four-wave mixing process as taking place in two steps: (1) absorption of two photons from the pump beam to reach the K_0 biexciton state and (2) deexcitation of the biexciton by the emission of two photons. The presence of the test beam causes the stimulated emission of a k_{-1} photon, along with a k_1 photon to satisfy energy and momentum conservation. Thus when this stimulated emission is stronger than the linear and the induced absorption of the test beam, a net amplification is observed.

The transmission spectrum of the test beam can be obtained by solving the propagation equations (2.16) for the pump and test beams,

$$\frac{\partial E_0}{\partial z}=\frac{i\omega}{c}[\epsilon_0(E_0)]^{1/2}E_0\ , \tag{3.14a}$$

$$\frac{\partial E_{-1}}{\partial z}=\frac{i\omega}{c}[\epsilon_{-1}(E_0)]^{1/2}E_{-1} \tag{3.14b}$$

for each frequency ω, and setting as a boundary condition that at $z=0$ the internal field is related to the incident intensity according to Eq. (3.10) self-consistently. In Eq. (3.14b) we have neglected the four-wave mixing term η_{-1} for the generation of the test beam, because of assumption (3.2). Equations (3.14) can be solved sequentially: the pump-beam equation can be solved as in paper I and its results can be inserted in Eq. (3.14b) to give the transmission of the test beam. Figure 4 presents the transmission spectrum of the test beam in the presence of the pump beam, obtained through the numerical solution of Eqs. (3.14). We note that the transmission spectrum of the test beam displays an intensity-dependent width which reflects essentially the chirping due to the attenuation of the pump beam, as described in paper I: As the pump beam is attenuated in the sample, the absorption maximum for the test beam shifts to higher frequencies due to the intensity dependence in the denominator of the susceptibility [Eq. (3.8)], thus giving an apparent width to the transmission spectrum. It is thus possible that the pump-induced absorption width of a pair of weak counter-propagating test beams recently reported[2] may be due (at least in part) to this chirping effect, rather than to collisional effects arising from the injection of polaritons and biexcitons by the pump beam.

The spectrum of the signal beam generated by the four-wave mixing process can be obtained by solving the propagation equation for that beam

$$\frac{\partial E_1}{\partial z}=i\frac{\omega}{c}[\epsilon_1(E_0)]^{1/2}E_1+4\pi i\frac{\omega}{c}\frac{\eta_1}{[\epsilon_1(E_0)]^{1/2}} \tag{3.15}$$

for each frequency, after inserting the results of Eqs. (3.14). A numerical solution as a function of frequency is presented in Fig. 5 for $I=2$ MW/cm^2, $\gamma=0.07$ and $\Gamma=0.15$ meV, and a CuCl slab thickness of 80 μm. This figure reproduces rather well the experimental observations of Ref. 3 including the strong asymmetry observed in the four-wave mixing spectrum. This latter feature can be explained within our model if we consider the fact that the four-wave mixing spectrum can be regarded to a first approximation as the superposition of two spectra: the spectrum for the generation of the signal beam, *minus* the absorption spectra for the pump, test, and signal beams. As shown in Fig. 6, the spectral maximum of the source term η_1 of the propagation equation lies to lower frequencies with respect to the absorption maximum given by the imaginary part of the susceptibility χ_1. When the two spectra are superimposed, the absorption carves out a dip on the side of the generation curve, thus giving an asymmetric appearance to the four-wave mixing spectrum. In addition the effects of the chirping due to the pump-beam attenuation, discussed above, as well as the linear absorption tend to enhance this asymmetry. At higher intensities, the frequency difference between the maximum of η_1 and χ_1 increases, and thus the absorption dip is produced further away from the peak of η_1. This causes an increase in the asymmetry of the four-wave mixing spectrum, in accordance with what was observed experimentally.[3] On the other hand, at sufficiently low pump intensities and for short distances of propagation the induced absorption is not very strong and no dip occurs in the four-wave mix-

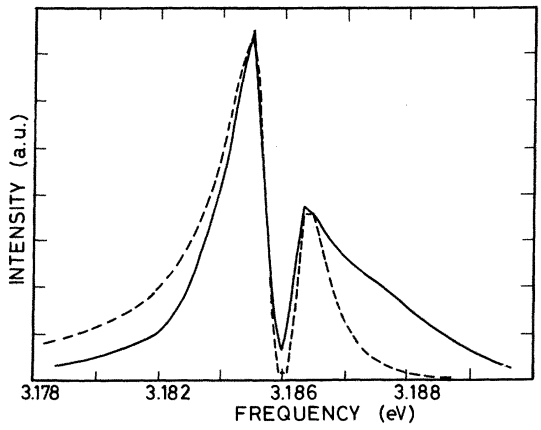

FIG. 5. Calculated (- - - -) and observed (——) spectrum of degenerate four-wave mixing signal near the two-photon biexciton resonance in a 80-μm slab of CuCl. For the calculated spectrum, pump intensity is 2 MW/cm^2 and damping constants are $\gamma=0.07$ and $\Gamma=0.15$ meV. Experimental spectrum taken from Ref. 3.

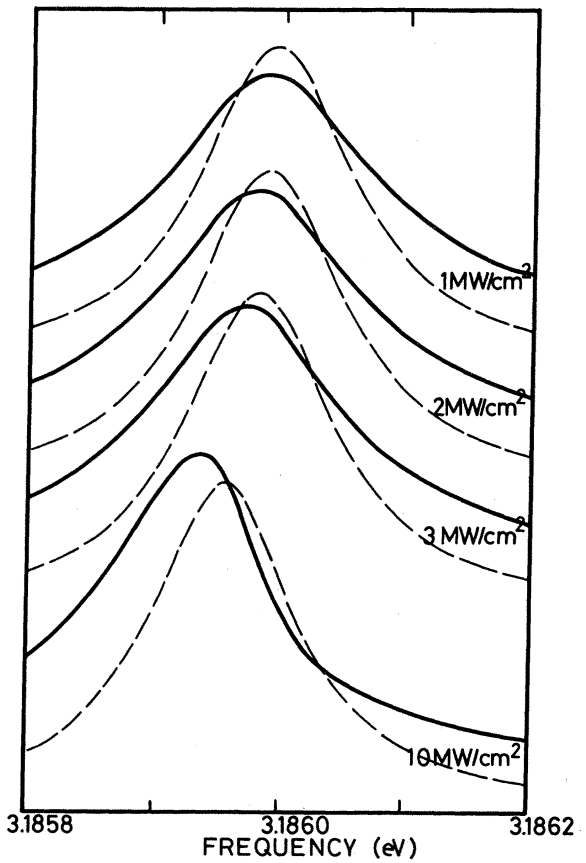

FIG. 6. Relative spectral positions of the renormalized signal generation term η_1 (——) and induced test and signal absorption Imχ_1 (— — —) in the degenerate forward four-wave mixing configurations. Curves are for different pump intensities. Spectral maximum of source term is always to the red of absorption maximum, giving rise to the asymmetry of the four-wave mixing spectrum in Fig. 5.

ing spectrum, a feature also observed experimentally. This strongly suggests that the spectral characteristics of the four-wave mixing signal must not necessarily be taken as evidence of a Fano interference between the sharp biexciton state and the two-polariton continuum as previously asserted.[3] The work of other authors[4,13] suggests that the Fano-interference model may even be at variance with the available data on the nonlinear-optical behavior of biexcitons.

Another feature of the calculated spectra which deserves some discussion is the values of the parameters for which these spectra fit the experimental data best. The only adjustable parameters were (1) the exciton damping constant found to be $\gamma\sim0.07$ meV and (2) the biexciton damping constant, with $\Gamma=0.15$ giving the best results. We note that the γ obtained is almost an order of magnitude smaller than that given by experiments in linear optics.[10] Such large values of γ cannot give a reasonable fit with the experimental four-wave mixing spectrum since the asymmetry is a very sensitive function of the exciton damping constant in our model. This large discrepancy can be understood if we consider the role of inhomogeneous broadening: Different microscopic regions in the crystal may have slightly different transition energies due to a distribution of random strains in the sample. The observed spectrum therefore will consist of a superposition of many "local" spectra slightly displaced with respect to each other, thus exhibiting an apparent "inhomogeneous" width. In a linear spectrum both the exciton damping and the inhomogeneity contribute to the experimental linewidth of the transition, and the two contributions cannot be disentangled without recourse to nonlinear techniques such as hole burning or photon echoes. In four-wave mixing, on the other hand, the damping constants and the inhomogeneity do not affect the spectral parameters in the same way: For example, the asymmetry of the four-wave mixing spectrum is not greatly modified by the presence of an inhomogeneous distribution and thus it may give access to a better determination of the exciton-damping constant. The small value of γ obtained is reasonable, given the small radius of the Z_3 exciton in CuCl: The lifetime (or coherence time) of the exciton is long, since there are few impurities or defects within its volume which could destroy the electron-hole correlation. The magnitudes of the values for both the exciton and biexciton damping constants are corroborated also by other nonlinear-optical experiments.[11]

The values obtained for the two damping constants are essentially indicative of their order of magnitude but are probably not very accurate. The reason is that the model used incorporates the main physical ideas behind the nonperturbational treatment of four-wave mixing but is certainly not complete: it treats the test and signal electric fields only to first order, neglects higher-order scattered beams, and does not include explicitly the role of inhomogeneous broadening and of the spectral bandwidth of the light beams. Inclusion of all these considerations would probably modify somewhat the values of γ and Γ that best describe the experimental spectrum. Extension of the model along these lines is possible within our formalism. The algebra, however, becomes quite cumbersome without much additional physical insight as a compensation.

IV. SUMMARY AND CONCLUSIONS

The near-resonant conditions and the giant oscillator strength of the exciton-biexciton transition render invalid the perturbational formulation of the nonlinear-optical response of CuCl near its two-photon biexciton resonance since the successive orders of the optical susceptibility diverge due to their resonant denominators. In paper I we developed a model which permits the nonperturbational calculation of the nonlinear-optical response of an exciton-biexciton system to a single laser beam, thus describing the nonlinear propagation of light in such a system. The model is based on a quantum-mechanical description of excitons and biexcitons as bosons while the electromagnetic field is treated classically, and the antiresonant terms of the radiative interaction are neglected. The corresponding Hamiltonian may be diagonalized analytically and this permits one to obtain the fully resonant part of the induced polarization nonperturbationally. The induced polarization displays a "biexciton" resonance whose position depends on the incident intensity. This implies that the transmission spectrum displays an intensity-dependent width in agreement with experimental observation: Attenuation of the propagating beam shifts the biexciton resonance frequency and thus gives rise to an apparent width due to the chirped absorption.

In this paper we extended the theory of paper I to account for multibeam experiments by including in the Hamiltonian the radiative interaction of all excitons and biexcitons whose wave vectors conform to the geometry imposed by the experimental configuration of the laser beams. To make contact with experimental observation we specialized our treatment to the case of forward degenerate four-wave mixing (in which a strong pump beam interacts with a weak test beam to produce a phase-conjugate signal beam) in a CuCl crystal with no initial population of excitons and biexcitons. The unitary transformation that diagonalizes this Hamiltonian can be obtained analytically through the solution of a system of linear equations, and this gives directly the induced polarization of the system.

The induced polarization thus obtained interacts with the incident radiation similar to a classical oscillating dipole antenna, as described by the Maxwell equations. For the sake of clarity, two contributions may be distinguished in the induced polarization for each wave vector k, which are respectively independent or depend on the electric field strength of the laser beam with the same wave vector k. The former serves as a source term for the generation of radiation of wave vector k and it corresponds to the renormalization of the third-order susceptibility for four-wave mixing by higher $(2n+1)$th order susceptibilities due to the high incident intensities. The latter term corresponds to the renormalization of the linear susceptibility for each beam by higher orders, and thus it gives rise to an effective dielectric function which each beam feels as it propagates in the sample in the presence of all other beams. The incident fields thus induce an anisotropy in the material system, since to each direction there corresponds a (generally) different dielectric function, arising from high-order interactions among the different propagating beams. In multibeam situations, therefore, it is not possible to characterize the optical response of the material system by a single effective dielectric function. Renormalization produces a qualitatively different dispersion relation for each beam. In particular, in the four-wave mixing configuration dispersion measurements performed on the weak test beam will indicate that the presence of the strong pump beam causes the opening of a polaritonlike forbidden gap in the vicinity of the two-photon biexciton resonance, its width and exact position depending on the intensity of the pump beam. On the other hand, the polariton dispersion experienced by the pump beam itself has a qualitatively different structure near the two-photon biexciton resonance: The effective refractive index presents a divergence at only one frequency and no polaritonlike gap opens up. When damping is included both the induced polariton gap (of the test beam) and the dispersion divergence (of the pump beam) disappear and the susceptibility acquires an imaginary part. For the pump beam this imaginary part is always positive indicating that the pump beam is attenuated upon propagation, while for the test beam it may have also negative values corresponding to an amplification upon propagation: Indeed, four-wave mixing involves the disappearance of two-pump photons simultaneous with the appearance of a test and a signal photon leading to a possible amplification of the test beam.

When the pump and test beams propagate simultaneously in the nonlinear medium, a signal beam is generated by four-wave mixing. The generation and propagation of this beam may be accounted for through the corresponding induced polarization and the Maxwell equations: the spectrum of the signal beam may be described roughly by the spectrum of the source term of the induced polarization, however, with a dip carved out because of the two-photon absorption of the pump beam and the pump-induced absorption of the test and signal beams. Since the spectral peak of the source term lies to the red of the two-photon absorption peak, the spectrum of the signal beam displays a marked asymmetry: it is more intense on the red side of the two-photon absorption dip, rather than on the blue side. This behavior has been observed also experimentally. In the initial interpretation of these experiments an autoionization of the biexcitons leading to a Fano interference was invoked in order to reconcile the observed asymmetry with a source term given only by the third-order nonlinear susceptibility $\chi^{(3)}$. However, the fact that a nonperturbational description of the optical response of biexcitons is necessary near resonance, together with the success of the nonperturbational calculation in accounting for the asymmetry of the four-wave mixing spectrum, does not permit us to deduce such an autoionization in biexcitons.

ACKNOWLEDGMENT

Thanks are due to Dr. A. Maruani for many helpful discussions.

*Laboratoire No. 250 associe au Centre National de la Recherche Scientifique.

[1]C. Klingshirn and H. Haug, Phys. Rep. 70, 316 (1981); D. S. Chemla and A. Maruani, Prog. Quantum Electron. 8, 1 (1982).

[2]L. L. Chase, N. Peyghambarian, G. Grynberg, and A. Mysyrowicz, Opt. Commun. 28, 189 (1979); N. Peyghambarian, L. L. Chase, and A. Mysyrowicz, *ibid.* 42, 51 (1982).

[3]A. Maruani and D. S. Chemla, Phys. Rev. B 23, 841 (1981); A. Maruani, Ph.D. thesis, University of Paris VII, 1981 (unpublished).

[4]D. S. Chemla, A. Maruani, and F. Bonnouvrier, Phys. Rev. A 26, 3026 (1982).

[5]R. März, S. Schmitt-Rink, and H. Haug, Z. Phys. B 40, 9 (1980); S. Schmitt-Rink and H. Haug, Phys. Status Solidi B 108, 377 (1981).

[6]F. Henneberger and V. May, Phys. Status Solidi 5, 133 (1983).

[7]I. Abram, Phys. Rev. B 28, 4433 (1983).

[8]B. Dick and R. M. Hochstrasser, Chem. Phys. 75, 133 (1983).

[9]D. P. Weitekamp, K. Duppen, and D. A. Wiersma, Phys. Rev. A 27, 3089 (1982).

[10]B. Sermage, M. Voos, and C. Schwab, Phys. Rev. B 20, 3245 (1979).

[11]Vu Duy Phach, A. Bivas, B. Hönerlage, and J. B. Grun, Phys. Status Solidi B 84, 731 (1977).

[12]J. B. Grun, B. Hönerlage, and R. Levy, Solid State Commun. 46, 51 (1983).

[13]Y. Masumoto and S. Shionoya, Solid State Commun. 38, 865 (1981).